A Near-sensor ECG Delineation and Arrhythmia Classification System

Xiaochen Tang, *Member, IEEE*, Shanshan Liu, *Member, IEEE*, Pedro Reviriego, *Senior Member, IEEE*, Fabrizio Lombardi, *Life Fellow, IEEE*, and Wei Tang, *Member, IEEE*

***Abstract*— Cardiovascular disease (CVD) has become the leading cause of death worldwide. As a widely used method for diagnosing CVD, currently electrocardiogram (ECG) monitoring tends to be implemented in wearable devices. This paper presents the prototype an ECG delineation and arrhythmia classification (EDAC) system suitable for wearable ECG biosensors. The proposed EDAC system is intended to be implemented after the electrodes and the analog front-end circuit, and its aim is signal processing at a low hardware overhead. The system consists of a Delta-modulator-based analog-to-feature converter (AFC), a corresponding ECG detection/delineation/feature extraction algorithm (DDF), an automatic gain controller (AGC) block, and a patient-dependent linear kernel support vector machine (SVM) classifier. The AFC converts the input analog signal into digital data of the slope and slope variation of the input signal, which is then used for detecting QRS complexes, localizing the fiducial points, and extracting the feature vectors for each heartbeat in the DDF block. At the same time, the AGC sends out a gain control signal based on the detected QRS complex to adjust the gain of the front-end amplifier. Finally, the SVM block performs arrhythmia classification. The EDAC system performance is evaluated using the MIT-BIH arrhythmia database. The system achieves 0.88% (0.93%), 99.1% (99.1%), 87.0% (92.8%), 99.6% (99.5%), and 89.3% (92.9%) in F1 score, accuracy, sensitivity, specificity, and positive predictive values of the supraventricular ectopic beats (ventricular ectopic beats) versus normal heartbeats classification while maintaining a low power dissipation (1.66 μW at 1kHz operating frequency in the front-end AFC block). The proposed system is attractive to future wearable long-term ECG monitoring biosensors.**

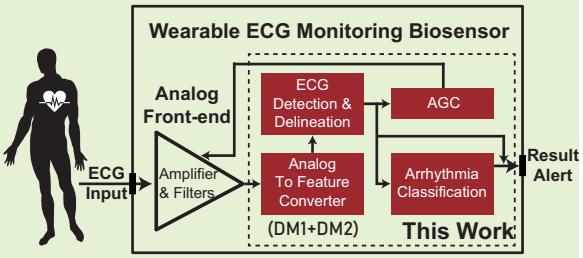

***Index Terms*— Electrocardiogram, Analog-to-feature converter, Delineation, Arrhythmia classification, Support vector machine**

I. Introduction

ACCORDING to the world health organization (WHO) [1], 32% of the total worldwide deaths are caused by cardiovascular disease (CVD). The American Heart Association (AHA) also reports that the estimated direct and indirect CVD expenditures are significant per year (e.g., $363.4 billion in 2016-2017) [2]. Therefore, there is an urgent need for early diagnosis techniques for CVD, which could significantly reduce mortality and expenditures. Electrocardiogram (ECG) monitoring for arrhythmia classification is an important tool for CVD diagnosis. The conventional clinical diagnosis utilizes a Holter monitor to record ECG data of the patients [3] so that doctors can diagnose and classify different arrhythmia types for further treatment. However, the Holter monitor is bulky and can only record data for 24 to 48 hours. Doctors can only diagnose after the recording period by fetching and analyzing all data. Nevertheless, an acute symptom that occurs during the ECG recording is still dangerous and may threaten the patient's life since the signal cannot be observed by the doctor in real-time.

An alternative class of ECG monitoring devices is wearable biosensors, for example, in steering wheels for driving [4], in armbands [5] or skintight T-shirts [6] for exercising, and typical electrodes placement on the chest [7]–[9]. They provide assistance for long-term ECG monitoring and can conduct *in-vitro* and continuous ECG measurements through low-power integrated circuit and system designs [10]. There are two main types of ECG monitoring biosensors found in the technical literature. The first type includes a low-power analog front-end and a radio frequency (RF) transmitter [11]–[13] that transmits all monitored data (i.e., raw data) to a remote station for arrhythmia classification. However, the RF part is typically the most power-consuming unit in the system, so the transmission of all data wastes a significant amount of power, because most data may not show anomalies. Another type of ECG monitoring device has additional near-sensor

This work was supported by United States National Science Foundation under Grant ECCS-1652944 and ECCS-2015573. (Corresponding author: Wei Tang.)

Xiaochen Tang, Shanshan Liu, and Wei Tang are with the Klipsch School of Electrical and Computer Engineering, New Mexico State University, Las Cruces, NM 88003 USA (e-mail: hypnus@nmsu.edu; ssliu@nmsu.edu; wtang@nmsu.edu).

Pedro Reviriego is with the Universidad Carlos III de Madrid, 28911 Leganés, Spain (e-mail: revirieg@it.uc3m.es).

Fabrizio Lombardi is with the Northeastern University, Department of ECE, Boston, MA 02115 USA (e-mail: lombardi@ece.neu.edu).

signal processing functions, such as heartbeat detection and partial arrhythmia classification [14]–[16]. In this case, a near-sensor arrhythmia classification is performed, only abnormal heartbeats are transmitted, so reducing system power for data transmission. The challenge of such a system comes from the computing and power overhead associated with the near-sensor signal processing circuits and algorithms.

Machine Learning (ML) has provided attractive solutions for performing arrhythmia classifications. For example, deep neural network (DNN) [16]–[18], long short-term memory (LSTM) [19], convolutional neural network (CNN) [20], [21], combining CNN with LSTM [22], recurrent neural network (RNN) [23], combining CNN with RNN [24], event-driven artificial neural network (ANN) [25], multi-layer perceptron (MLP) combined with CNN [26], and support vector machine (SVM) with linear kernels [27], [28], non-linear kernels [29], [30], and combining SVM with random forest (RF) and k-nearest neighbors (KNN) classifiers [21] have been proposed for remote diagnosis. However, without a preliminary step of ECG delineation-based feature extraction, these ML algorithms typically incur high hardware complexity as they must perform continuous time series classification using raw ECG data. This poses a critical issue when implementing ML-based classification in ECG monitoring biosensor systems with strict requirements on power and battery endurance. However, existing ECG delineation methods are also difficult to be implemented because using near-sensor processing units, the detection of critical waves in the ECG waveform (e.g., P waves with significantly low amplitude) usually applies the wavelet transform that has a high computational complexity [27], [28], [31].

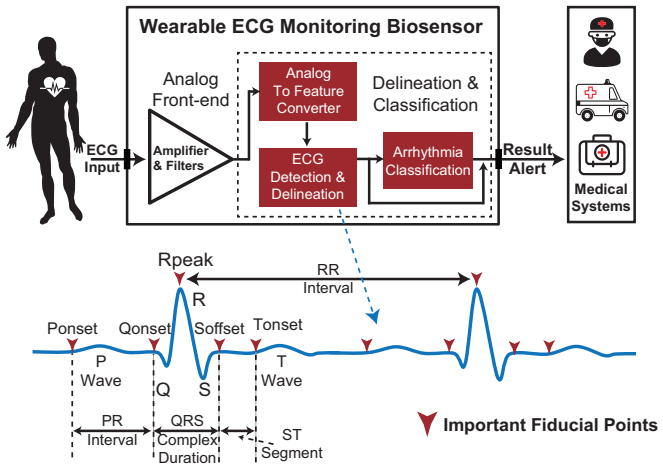

Fig. 1. Illustration of a wearable ECG monitoring device with near-sensor delineation and arrhythmia classification (the scope of this work is marked by the dashed block).

To address these issues, Delta modulator-based analog-to-feature converter (AFC) chips have been designed for performing feature extraction from the ECG data as per our prior works [32], [33]. Once these features are extracted, a patient-dependent rotated linear kernel SVM classifier has been designed for classifying different types of abnormal heartbeat [34]. Since a few critical features are extracted prior to arrhythmia classification, the computational complexity of the SVM algorithm is significantly reduced. Nevertheless, even though such an ECG delineation and arrhythmia classification (EDAC) system provides acceptable classification performance at low-power dissipation as validated in many cases using the MIT-BIH arrhythmia database [35], [36], there are two major limitations in prior EDAC designs that may degrade the classification performance:

1) In existing AFCs, features are selected primarily based only on the morphology of the essential waves [34], or the timing of fiducial points [33]. The unbalanced feature selection may harm classifying certain types of heartbeat. Compared with other feature extraction methods (that use wavelet coefficients as features), the essence of the feature selection process also remains unclear;
2) For features extracted from some ECG data that have significant amplitude variations (as commonly found in practice), the existing AFCs lack automatic gain control (AGC) and cannot generate satisfactory results.

All these issues may finally lead to an incorrect classification when subsequently executing the SVM algorithm.

Therefore, this paper is an extension of our earlier work in [32], [33]. In this paper, an improved EDAC system is proposed. The goal is to achieve balanced extracted features and perform classification while maintaining low power dissipation. The significant contributions of this paper are summarized as follows:

1) A novel AFC is proposed to generate a comprehensive set of features, it generates both slope and slope variation information of the input ECG signal. The obtained features include QRS complex morphology and timing of important fiducial points of the ECG signal.
2) An R wave slope variation sensitive AGC design is proposed. It operates with the QRS detection algorithm and alleviates the issue of amplitude variation of the ECG signals to generate high-quality features.
3) Two importance scores are proposed, and the importance of different ECG features used for performing classification is analyzed by considering these two scores. Compared with prior methods, this analysis provides a more informative emphasis on feature selection when classifying supraventricular ectopic beats (SVEB) and ventricular ectopic beats (VEB). They are of considerable benefit to future ECG monitoring biosensor system design.

The rest of this paper is organized as follows. First, the most relevant related work is briefly discussed in Section II. Then Section III describes the proposed system and the details of each block. The system performance is evaluated in terms of QRS detection, hardware power dissipation, and arrhythmia classification in Section IV. Section V analyzes and discusses the importance of features using two proposed importance scores. Limitations and future perspectives of this work are discussed in Section VI. Finally, Section VII concludes the paper.

II. Preliminaries

A typical wearable ECG monitoring biosensor with a near-sensor machine-learning-based algorithm is depicted in Fig. 1, it consists of a low-power analog front-end (AFE), and an EDAC system [33]. The analog front-end performs noise filtering and amplification, and the AFC block performs the analog-to-digital conversion and extracts critical features in the digital format for the next stage of processing in the EDAC system. In particular, the AFC block converts the input analog signal into digital features in the form of a bitstream. Then, the ECG detection and delineation block processes the digital bitstream to detect critical ECG fiducial points, including the P wave, the QRS complex, and the T waves. Such information is important for abnormal heartbeat delineation [35]) as shown in Fig. 1. As per such information, the shapes (e.g., slope variations) and essential intervals (e.g., the PR/RR interval, $etc.$) of the ECG signals are then extracted to form the final features.

The subsequent heartbeat classification is performed in the arrhythmia classification block, in which a low-complexity ML algorithm such as a patient-dependent SVM classifier [34] is implemented. If the captured ECG signal is finally classified as a type of arrhythmia (e.g., SVEB or VEB), an alert signal should be generated to trigger further attention in the remote station for timely diagnosis or treatment. Thus, instead of sending all raw data, only the important episode of ECG data around the anomalies is recorded and transmitted to the remote station for further analysis. Due to the significant reduction in the transmitted data volume and the required power dissipation, the system is expected to monitor ECG continuously for long periods of time. The primary challenge of the system comes from the amplitude variation of the ECG signals, which may result in inconsistent feature extraction for the same type of heartbeats and introduce unnecessary disturbing data for arrhythmia classification. Such issues may cause incorrect classifications and thus, it constrains the applicability of the system.

III. Proposed System

In this paper, an improved EDAC system is proposed for achieving a comprehensive feature extraction that leads to a better classification performance compared to existing designs, while maintaining a low power dissipation. Except the significant contributions mentioned above, the design of the proposed system utilizes the new ECG delineation algorithm based on the new AFC. Moreover, it has implemented the output interface, and achieved new arrhythmia classification models. Fig. 2 shows the proposed EDAC system. Individual functional blocks are described in detail in this section.

A. Delta modulator based AFC

As shown in Fig. 2, compared with prior AFC designs that are realized by the parallel first-order delta modulator (DM1) [32] or parallel second-order delta modulator (DM2) [33], the proposed AFC circuit is composed of one DM1 and the parallel DM2 blocks. The DM1 chip converts the analog input signal to its slope information and is fabricated using standard 0.13 μm CMOS technology with a 360 nW power dissipation. The DM2 chip extracts the slope variation information of the input and is fabricated with standard 0.18 μm CMOS technology with a 151 nW/channel power dissipation. Both DM1 and DM2 are designed using an operational transconductance amplifier (OTA) based switched-capacitor discrete-time integrator. The integrator is controlled by non-overlapping clocks ($\phi_{1,2,1e,2e,cmp}$) to form the negative feedback. The residue voltage on the capacitor (Csub) is the subtraction result between the feedback and the input, and is compared with the thresholds (ThreshH, ThreshL) through a ternary comparator (Ternary Comp). After that, the output bits pair ($+1$, -1 channel) of the current clock are generated. Since two blocks extracting the different feature information are combined, the proposed AFC provides a comprehensive feature extraction ability. This is analyzed next by considering the example given in Fig. 3.

A standard ECG signal is processed by using the proposed AFC as shown in Fig. 3. Since the pulse density in the output bitstream of DM1 should be proportional to the slope of the input signal, its output pulses are mainly concentrated in the QR segment and the RS segment that contain the steepest slope portion of the ECG signal. Therefore, we can obtain the slope information features from this segment in DM1 as shown in the dashed block of Fig. 3. At the same time, DM2 is sensitive to the turning points of the input signal (i.e., the Q/R/S wave peaks) that contain the most significant slope variations of the input. Therefore, its output pulses are more intensive around these peak locations. As per this information, timing features are extracted on the fiducial points (Fig. 3, dashed block). To achieve a more accurate QRS detection, two parallel DM2 (namely DM2_qrs and DM2_pt) are employed in the proposed AFC. As shown in Fig. 3, DM2_qrs detects significant slope variations such as QRS complexes that usually have large amplitudes. Meanwhile, DM2_pt reacts to all small waves. DM2_pt cannot detect large waves since it may fall in saturation conditions and result in long consecutive +1/-1 bitstreams).

B. ECG detection/delineation and feature extraction (DDF)

To perform near-sensor arrhythmia classification, low-complexity feature extraction circuits are expected to work prior to sending information to the classifier. Otherwise, the system would consume significant power if the classifier processes the raw digital data directly, which is unacceptable for wearable devices [17]. To perform ECG delineation, the detection of the QRS complex must be first achieved. In the DDF block of the proposed system, this is performed by analyzing the output bitstream of DM2 as shown in Fig. 2, in particular the result of DM2_qrs. By taking advantage of DM2_qrs's sensitivity to upward/downward turning points (UTP/DTP, defined as +1/-1 pulses in Fig. 3), and setting a defined timing window (Wdef) and a turning point detection threshold (TPDTh, defined as the number of pulses [33]), the QRS complex can be detected once a UTP-DTP-UTP pattern is recognized in the bitstream. At the same time, the values of the slope variation at these points are also recorded. Note that

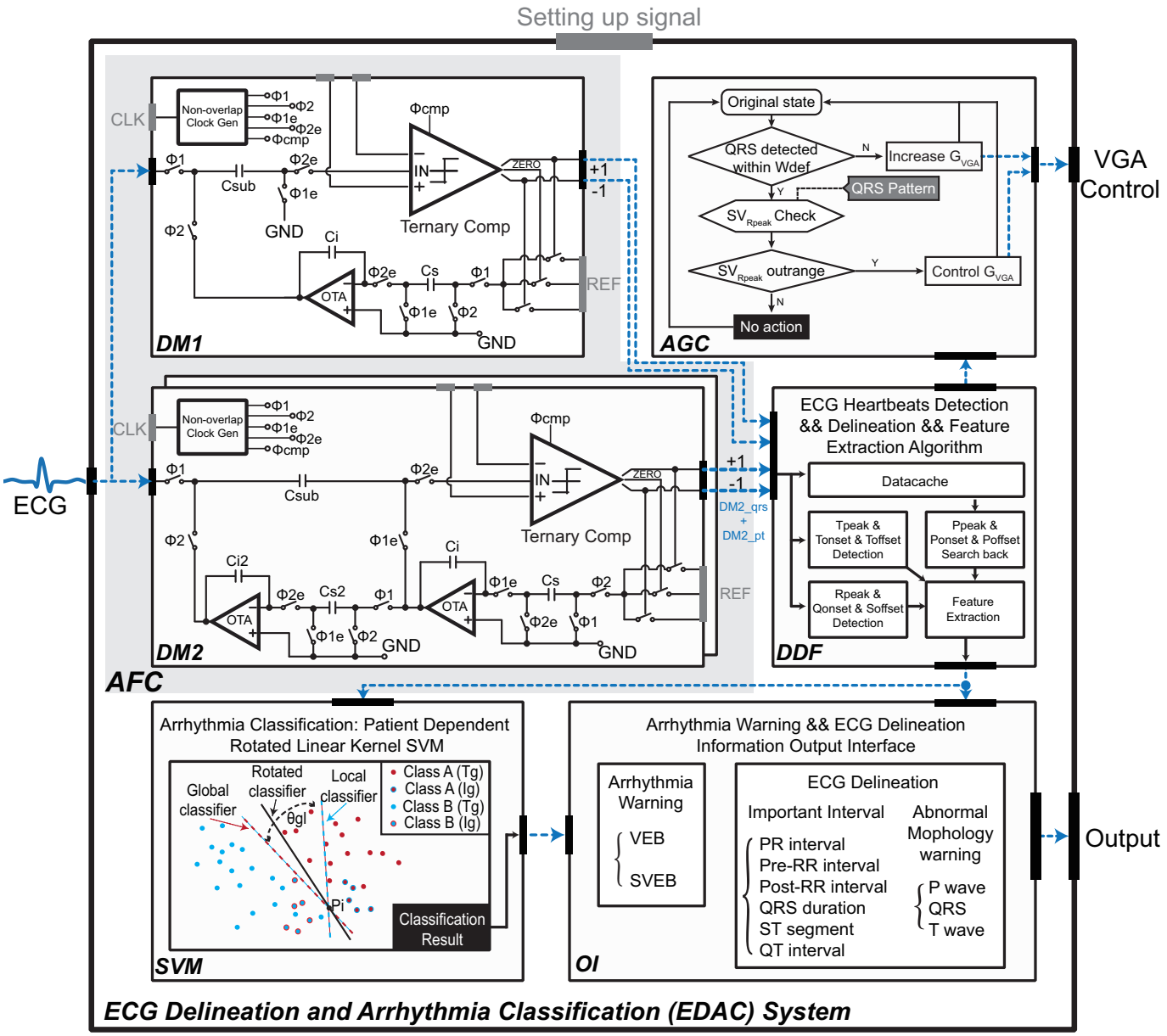

Fig. 2. The proposed EDAC system includes an AFC that consists of a DM1 and the parallel DM2, an AGC, an ECG detection/delineation/feature extraction algorithm (DDF), a patient-dependent SVM classifier (SVM), and an output interface (OI) that reports warnings and fiducial points).

abnormal QRS complexes with different morphology forms can be detected in parallel by checking different data patterns. For example, for a common form of premature ventricular contraction (PVC) heartbeat, the pattern of DTP-UTP-DTP is used for QRS complex detection. In another case, in an ECG wave with baseline wandering or wave morphology change caused by the sensor placement issue, the typical UTP-DTP-UTP pattern can be used but with a TPDTh setting to different values. This QRS complex detection process is enabled if no heartbeat is detected within a certain-bits window in the proposed design. For example, Wdef is set to twice the averaged RR interval as default.

Once the QRS complex is detected, the delineation is performed by recording the timing information of the peaks of the Q/R/S waves, the onset of the Q wave, and the endpoint of the S wave from the bitstream of DM2_qrs. Following this method, the system searches back in the data cache to locate the fiducial points of the P wave and searches forward to detect these points of the T waves from the bitstream of DM2_pt to perform detection and delineation for these waves. Moreover, with the slope steepness features of the QRS complex extracted from the bitstream of DM1, the DDF block can extract 50 types of features in total as summarized in Table I. Combining DM1 and DM2 in the proposed AFC block, the features obtained in the DDF block are significantly more comprehensive compared to existing feature extraction methods, which is better assisting the subsequent arrhythmia classification.

C. QRS complex detection based AGC

To alleviate the influence issue of amplitude variation in ECG signals encountered by existing feature extraction meth-

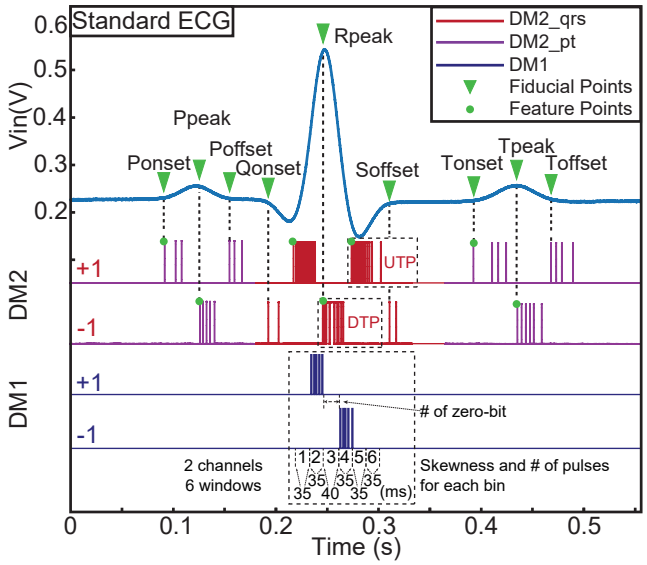

Fig. 3. Example of output bitstreams of the proposed AFC, including the DM2 bitstreams that detect turning points for feature extraction in both timing and morphology and the DM1 bitstreams that detect slope information (extracted from 6 bins each channel).

TABLE I
DESCRIPTION OF THE 50-ELEMENT FEATURE VECTOR

Feature Description	Category	# of Features	Source
Consecutive pulses weighted skewness (2 channel, 6 windows: Skewp.b1-b6, Skewn.b1-b6)	Morphology	12	DM1
Number of pulses in bitstream (2 channel, 6 windows: Pulsep.b1-b6, Pulsen.b1-b6)	Morphology	12	DM1
Number of Zeros bits during R peak (last +1 in QR, to first -1 in RS: Zerolength)	Morphology	1	DM1
Number of bits during QR/RS segment (+1 in QR, -1 in RS: QRlen, RSlen)	Morphology	2	DM1
Slope pattern (+/- or -/+: Skewpattern)	Morphology	1	DM2
Important waves morphology (P/T waves, QRS complex: P.morph, T.morph, QRS.morph)	Morphology	3	DM2
Turning points slope variation (SV.Pon/Ppk/Qpk/Rpk/Spk/Ton/Tpk)	Morphology	7	DM2
Intervals and segments (PonQon/PonQpk/PpkQpk/PpkRpk/ QonTpk/RpkTpk/SpkTon.interval, QR/RS/QRS.duration; RR intervals: RR.pre, RR.pos)	Timing	12	DM2

ods introduced previously, an automatic gain control (AGC) is designed in the proposed system to adjust the amplitude of the input signals as per the QRS complex detection result of the DDF block. As shown in the AGC block of Fig. 2, the AGC algorithm executes as follows: 1) Obtain the largest slope variation. When a QRS complex is detected, the AGC receives the related QRS complex pattern and checks the largest slope variation within the ECG signal, i.e., the R wave peak (SV.Rpeak); 2) Check the SV.Rpeak. If the SV.Rpeak is out of the defined range (SV.th), the AGC controls the gain of the VGA (G_{VGA}) and adjusts the amplitude of the subsequent input signal by uniforming the SV.Rpeak to SV.th. 3) No heartbeat detected condition. If no QRS complex is detected within the defined bits window Wdef (as shown in Fig. 2), the AGC assumes there is no sufficient gain. The AGC then communicates with the VGA to adjust the gain of the amplifier.

D. Patient-dependent SVM for arrhythmia classification

Performing arrhythmia classification is a challenge for ML algorithms due to the large interpatient and intrapatient variations of ECG morphology. The arrhythmia classifier employed in the proposed system follows the patient-dependent SVM classification algorithm from [37] to enhance performance for both the generalization and specificity using the comprehensive features generated by combining the DDF and AGC blocks. The MIT-BIH arrhythmia database is used for training and testing the classifier. According to the Association for the Advancement of Medical Instrumentation (AAMI) standard [38], heartbeats in the database are divided into five types, i.e., normal beats (N), SVEB, VEB, fusion beats (F), and unknown beats (Q). Except for the four data records from patients who carry pacemakers, 44 records are involved in training and testing the proposed classifier. The 44 records are separated into two groups: i) the training dataset that includes records 101, 106, 108, 109, 112, 114, 115, 116, 118, 119, 122, 124, 201, 203, 205, 207, 208, 209, 215, 220, 223, 230, ii) the inference dataset that includes records 100, 103, 105, 111, 113, 117, 121, 123, 200, 202, 210, 212, 213, 214, 219, 221, 222, 228, 231, 232, 233, 234 [39].

The 22-fold recording-by-recording cross-validation method proposed in [39] is utilized for assessing the classifier performance and finding the optimum rotation angle to be used for combining the global and the local classifiers. Then, the global classifier is trained using the training dataset. After that, the first 500 heartbeats in each record of the inference dataset and base data (records 209 and 215) are used for training the local classifier for each patient in the inference dataset. With the method of [34], the intersection hyperplane between the global and local classifiers can be determined by rotating the global classifier towards the local classifier at a proper angle. Therefore, both the specificity of the patient ECG and the generalization performance of the SVM classifier can be achieved.

E. Output interface (OI)

As shown in the OI block of Fig. 2, in addition to the arrhythmia classification result/warning for VEB and SVEB, the proposed system also reports the results of ECG delineation including information of important intervals and morphology of critical waves for abnormal heartbeats. They can be assessed by doctors for a more detailed analysis. Thus, by transmitting only the abnormal ECG data, the proposed system essentially reduces power dissipation for RF circuits, extends battery life, and reduces the burden of continuous technical analysis on extensive volume data received at a remote station.

IV. PERFORMANCE EVALUATION

To validate the functionality of the proposed EDAC system, a testbench is built as shown in Fig. 4. The testbench consists of the DM2/DM1 chips, an FPGA that is used for

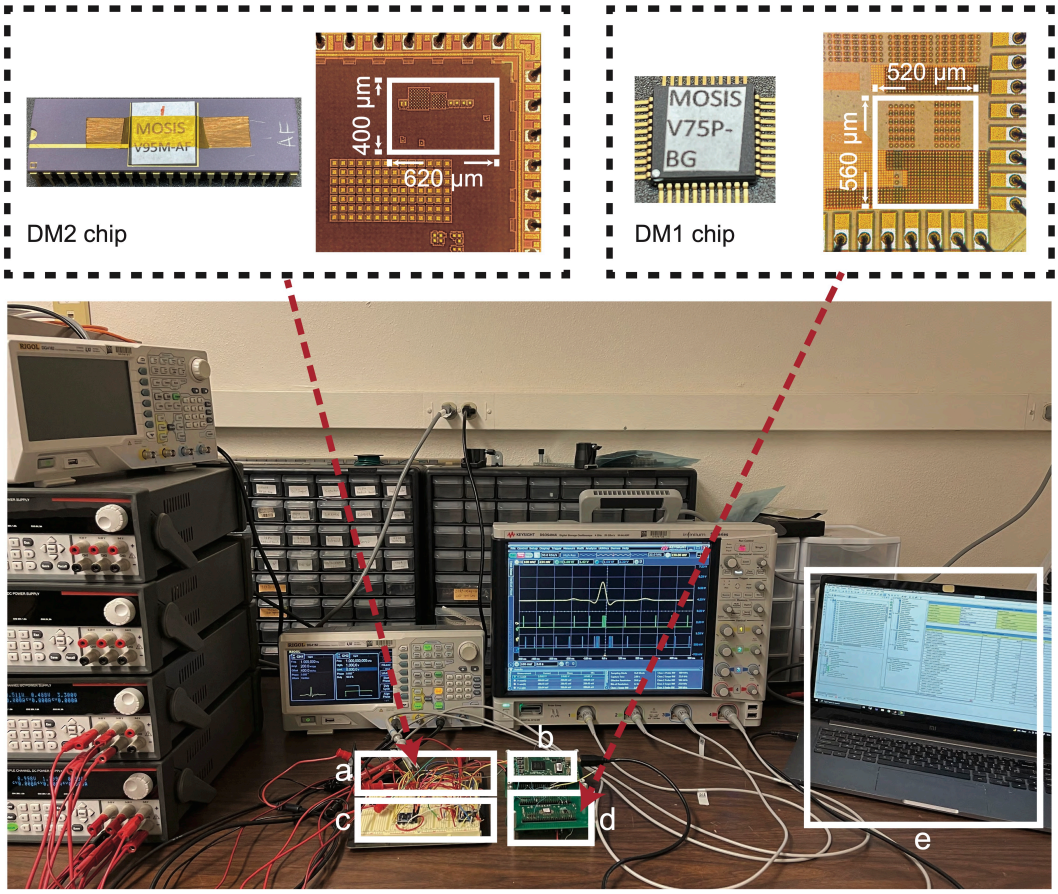

Fig. 4. The measurement of the proposed EDAC system. Top left: package and microphotograph of DM2 chip; Top right: package and microphotograph of DM1 chip; Bottom: testbench of the EDAC system (a: DM2, b: FPGA, c: peripheral circuits, d: DM1, e: PC platform).

corresponding algorithms implementation, peripheral circuits for connecting the electrodes and the EDAC system, and a PC for communicating with the FPGA. Since the proposed EDAC system targets the improvement of feature extraction and then arrhythmia classification while maintaining low power, these metrics are evaluated and compared in this section to existing works. The hardware testbench validates the functionality of the proposed analog to feature conversion system, while simulations are applied using the MIT-BIH database for evaluating the classification performance. Ethical approval for this work has been granted by the Office of Research Compliance of New Mexico State University.

A. QRS Detection Performance

Since some records in the MIT-BIH arrhythmia database have severe QRS complex amplitude variation such as record 106, which is also commonly occurring in practical ECG measurements, the proposed AGC is implemented to improve the performance of a heartbeat detection algorithm to handle such cases. Moreover, the feature extraction algorithm of the DDF block can also be benefited from the obtained unified-amplitude ECG signal using the AGC. For example, as shown in Fig. 5, the amplitude variation issue is significantly alleviated. For example, the false-negative beats (FN) reduce from 60 to 5 compared to a system without AGC [33]. This makes the FN decrease from 3.0% to 0.2%. Meanwhile, false-positive beats (FP) are not primarily affected (an increase from 2 to 4, i.e., from 0.1% to 0.2%).

The performance is compared between systems with and without an AGC. For example, the heartbeat detection strategy without an AGC in [33] uses a fixed amplification coefficient and tries to make most of the QRS complexes amplified to 0.2V for increasing the detection accuracy. This may result in a large number of normal heartbeats with abnormal amplitude while introducing difficulties for arrhythmia classification with features extracted from these normal "anomalies". The performance of the QRS detection algorithm with AGC is evaluated using the MIT-BIH arrhythmia database; as shown in Table II, the overall detection sensitivity (SE), the positive predictive value (PPV), and the detection error rate (ER) are 98.67%, 98.84%, and 2.49%, respectively. SE, PPV, ER are defined as per the following equations:

$$SE(\%) = \frac{TP}{TP + FN} \tag{1}$$

$$PPV(\%) = \frac{TP}{TP + FP} \tag{2}$$

$$ER(\%) = \frac{FN + FP}{TP + FN} \tag{3}$$

where TP is the number of true positive detection heartbeats.

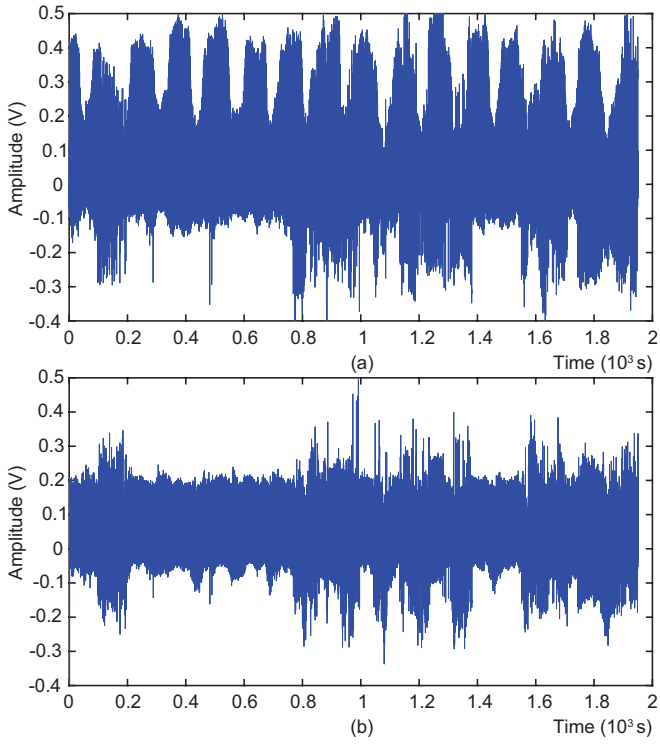

Fig. 5. The amplitude variation issue of record 106: (a) without AGC; (b) with AGC.

B. Arrhythmia classification

Targeting on the single lead arrhythmia classification (Modified Limb Lead II configuration for electrodes placement on chest), with the proposed comprehensive feature extraction method, we apply the patient-dependent SVM algorithm of [34] to perform arrhythmia classification, as for future hardware implementation. For example, it requires only 50 multiplications and 51 additions per classification, which is hardware efficient compared to other machine-learning-based algorithms. The overall classification performance is evaluated using the F1 score (F1), the classification accuracy (ACC), sensitivity (SE, usually the most significant metric), specificity (SP), and the positive predictive value (PPV); they are defined as per Eqs. (1), (2), (4) to (6) respectively.

$$F1 = \frac{2 \times TP}{2 \times TP + FP + FN} \tag{4}$$

$$ACC(\%) = \frac{TN + TP}{TN + TP + FN + FP} \tag{5}$$

$$SP(\%) = \frac{TN}{TP + FP} \tag{6}$$

The feature vector used in arrhythmia classification is generated from the DDF block, and only detected heartbeats in Table. II are involved. The average classification performance of different systems covering all considered data is shown in Table III. The proposed system achieves comparable performance to each of the best metrics among existing systems found in the technical literature [34], [37], [39], [40], [44], [48]–[50]:

TABLE II
QRS DETECTION PERFORMANCE OF THE PROPOSED SYSTEM

ID	Total	FN	FP	SE	PPV	ER
100	2273	1	1	99.96	99.96	0.09
101	1865	4	7	99.79	99.63	0.59
102	2187	4	5	99.82	99.77	0.41
103	2084	0	1	100.00	99.95	0.05
104	2229	66	35	97.04	98.41	4.53
105	2572	46	49	98.21	98.10	3.69
106	2027	5	4	99.75	99.80	0.44
107	2137	5	1	99.77	99.95	0.28
108	1763	323	331	81.68	81.31	37.10
109	2532	6	3	99.76	99.88	0.36
111	2124	5	16	99.76	99.25	0.99
112	2539	2	5	99.92	99.80	0.28
113	1795	1	1	99.94	99.94	0.11
114	1879	5	18	99.73	99.05	1.22
115	1953	0	1	100.00	99.95	0.05
116	2412	41	21	98.30	99.12	2.57
117	1535	1	3	99.93	99.80	0.26
118	2278	1	7	99.96	99.69	0.35
119	1987	1	4	99.95	99.80	0.25
121	1863	5	8	99.73	99.57	0.70
122	2476	2	3	99.92	99.88	0.20
123	1518	1	2	99.93	99.87	0.20
124	1619	4	2	99.75	99.88	0.37
200	2601	45	96	98.27	96.38	5.42
201	1963	46	29	97.66	98.51	3.82
202	2136	4	2	99.81	99.91	0.28
203	2980	116	146	96.11	95.15	8.79
205	2656	6	3	99.77	99.89	0.34
207	2332	366	114	84.31	94.52	20.58
208	2955	151	28	94.89	99.01	6.06
209	3005	10	18	99.67	99.40	0.93
210	2650	21	23	99.21	99.13	1.66
212	2748	4	9	99.85	99.67	0.47
213	3251	3	2	99.91	99.94	0.15
214	2262	7	5	99.69	99.78	0.53
215	3363	4	8	99.88	99.76	0.36
217	2208	6	5	99.73	99.77	0.50
219	2154	0	1	100.00	99.95	0.05
220	2048	0	0	100.00	100.00	0.00
221	2427	10	3	99.59	99.88	0.54
222	2483	76	88	96.94	96.47	6.60
223	2605	5	3	99.81	99.88	0.31
228	2053	37	137	98.20	93.64	8.48
230	2256	1	5	99.96	99.78	0.27
231	1571	1	3	99.94	99.81	0.25
232	1780	5	15	99.72	99.16	1.12
233	3079	9	5	99.71	99.84	0.45
234	2753	3	1	99.89	99.96	0.15
Total	109966	1465	1277	98.67	98.84	2.49

- Compared with [42] that has the best results for VEB classification, the proposed system achieves similar performance except for SE and PPV (5% less). [42] was achieved by deep learning, and it has three hidden layers with a structure 417–100–100–100–5. In addition, the proposed work performs better when classifying SVEB.
- Compared with [40] which performs the best in SVEB classification (considering especially SE that represents the classified SVEBs over total SVEBs), the proposed system also achieves comparable results, with a 3% reduction in PPV but it is still 1.5% better in SE. However, [40] utilizes a GPU-based classification algorithm, which is not fully applicable to wearable biosensors.

TABLE III
COMPARISON OF CLASSIFICATION PERFORMANCE AMONG DIFFERENT SYSTEM

Methods	SVEB					VEB				
	F1	ACC	SE	SP	PPV	F1	ACC	SE	SP	PPV
Li (2017) et.al [40]	**0.89**	**99.4**	85.5	99.4	92.3	0.90	98.9	88.0	98.9	92.6
Saadatnejad (2019) et.al [19]	0.87	98.6	75.2	**99.9**	**99.8**	0.97	99.3	96.0	99.8	**98.3**
Amirshahi (2019) et.al [41]	-	-	-	-	-	0.88	97.9	80.2	99.8	97.3
Xu (2019) et.al [42]	0.87	99.1	78.4	**99.9**	98.7	**0.98**	**99.7**	**97.4**	**99.9**	97.8
Wang (2019) et.al [26]	0.87	**99.4**	79.5	**99.9**	96.3	0.94	99.1	91.8	99.6	95.3
Tang (2019) et.al [34]	0.83	98.8	79.3	99.6	88.2	0.92	99.0	92.8	99.4	91.6
Malik (2021) et.al [43]	0.79	97.3	76.0	99.6	82.2	0.97	99.0	95.3	98.9	97.9
Tang (2021) et.al [44]	0.82	98.5	**88.8**	98.9	76.1	0.95	99.4	95.1	99.7	95.2
Proposed method	**0.88**	**99.1**	**87.0**	**99.6**	**89.3**	**0.93**	**99.1**	**92.8**	**99.5**	**92.9**

C. Power Dissipation and Hardware Overhead

One important metric for evaluating the wearable ECG monitor is the hardware overhead in terms of power dissipation and hardware complexity, which can be translated to the chip area. For the biosensor employing the proposed EDAC system, the DM1 and DM2 chips were fabricated using 130 nm and 180 nm standard CMOS technologies, respectively. Under an operating clock at 1 KHz, the power consumption of the AFC is measured as 602 nW. The other digital blocks (AGC, DDF, SVM, and OI) in the proposed system are designed using 180 nm standard CMOS technology, and chip area (0.4 mm^2) and power dissipation (1054 nW) are found using Synopsys Design Compiler. SVM models are trained on a PC platform using MATLAB.

Table IV compares different ECG biosensor systems. All compared systems can perform heartbeat detection, but only [46] and [44] can perform ECG delineation. [46] implements the delineation algorithm in a microcontroller (MCU) that consumes power at a mW level. Compared with a previous design [44], the PPV of the SVEB classification of the proposed system is greatly improved due to the proposed comprehensive AFC with AGC. Compared with [47] and [25] which provide the arrhythmia classification ability, the proposed system is implemented with lower-complexity algorithms, while achieving a good classification performance. Overall, the proposed system is more attractive for low-power near-sensor arrhythmia classifying scenarios.

V. IMPORTANCE OF FEATURES

Due to the higher quality of extracted features and the comprehensive strategy of feature selection using the proposed AFC and AGC, the proposed EDAC system achieves a balanced performance when classifying arrhythmia heartbeats, which is verified in Table III. For instance, when compared with [34] which uses only morphology-based features, the proposed EDAC achieves a significant improvement for SVEB classification on SE (from 79.3% to 87.0%). In another example, when compared with [44] which uses timing-based features, the proposed EDAC improves the SVEB classification on PPV from 76.1% to 89.3%.

The patient-dependent SVM classification algorithm of [34] is employed in the proposed EDAC system. The system has an extremely low computation complexity since it utilizes the linear kernel function. Such a function makes the feature importance analysis straightforward by sorting only the values of the weights (W_T) in each classifier (i.e., global and local classifier). However, as the values of the features may have different distributions, even though they are typically normalized, considering only W_T may result in an incorrect analysis of the feature importance. This may degrade performance when conducting a co-design between different blocks and circuits in terms of feature extraction and classification.

To address this issue, two novel feature importance scores IMP_G and IMP_L for feature selection of arrhythmia heartbeats classification studies are defined for evaluating the global and local classifier of the patient-dependent SVM algorithm, respectively. The linear kernel makes such feature importance analysis straightforward by sorting the value of the weights (W_T) in each SVM model. However, to remove the distribution of elements in feature vectors, IMP_G and IMP_L are defined using the following equations:

$$IMP_G = W_{T,Global} \cdot median(FV_{Global}) \tag{7}$$

$$IMP_L = \sum_{n=1}^{22,I_{data}} (W_{T,Local} \cdot median(FV_{Local}) \cdot \frac{N_{Target}}{N_{Total}}) \tag{8}$$

Here FV_{Global} and FV_{Local} are the feature vectors used in training the global and local classifiers. N_{Target} (N_{Total}) are the total number of arrhythmia heartbeats in each record. I_{data} denotes the inference dataset, and $median()$ finds the median of each element in the feature vectors set. Therefore, for both models, the use of $median()$ ensures to establish the essential features, which may be masked by considering only the weights. For example, for two normalized features that have the same weight, but feature values are distributed around different values, only sorting the weights cannot reveal the importance of the features. By adjusting the feature values using different normalization factors, the weights value also change. Additionally, for the local classifier, IMP_L covers all 22 records by involving $\frac{N_{Target}}{N_{Total}}$ and addresses the issue of variations in arrhythmia heartbeat number for different records.

The normalized feature importance for SVEB and VEB heartbeats classification is obtained by calculating the proposed two importance scores and are summarized in Fig. 6. The table shows that the RR intervals play essential roles in almost all models. Here the RR intervals include RR.pre which is the interval between the prior R peak and the current R peak, and RR.pos, which denotes the interval between the current R peak and the post R peak. The importance of features in SVEB classification shows a distinct difference between global and local classifiers. Morphology features extracted from DM1 are more critical in global models while features from DM2 are more important in the local models. This indicates that SVEB has more specific interpatient differences, and the RR intervals are significantly more critical in interpatient features. For VEB classification, the importance of features is close to the classification of SVEB. The distribution shows that VEB features are more balanced. For SVEB classification, there are seven same features in the top 20 critical features and one same feature in the top 10 critical features between the global

TABLE IV
COMPARISON OF HARDWARE OVERHEADS AMONG DIFFERENT ECG MONITORING DEVICES

		This work	[45] JSSC19	[46] JBHI18	[44] TBCAS21	[47] TCASII18	[25] TCASII21
Function*		1-5	2	1-4	1-5	2, 5	2, 5
Method	Processing	Comprehensive Delta Modulator	Proportional Derivative Control	Second Derivative + FIR Filter	Second Order Delta Modulator	Wavelet	Level Crossing
	Classification	Rotated SVM	-	-	Rotated SVM	Hybrid SVM	ANN
Technology (nm)		180+130	65	MCU	180	40	180
Power Supply (V)		1.0	0.55	3.7	1.0	1.1	1.5
Frequency	Sampling (KS/s)	1	0.25	0.25	1	0.36	0.36
	Operating (KHz)	1	2	8000	1	10	250
Power Dissipation (μW)		1.66	1.06	1145	0.302 + FPGA	3.76	1.3
Area (mm^2)		0.63	1.5	-	0.29	0.12	0.75

* Functions: (1) P wave detection; (2) R wave detection); (3) T wave detection; (4) onset/offset detection of P/T wave and QRS complex; (5) arrhythmia classification.

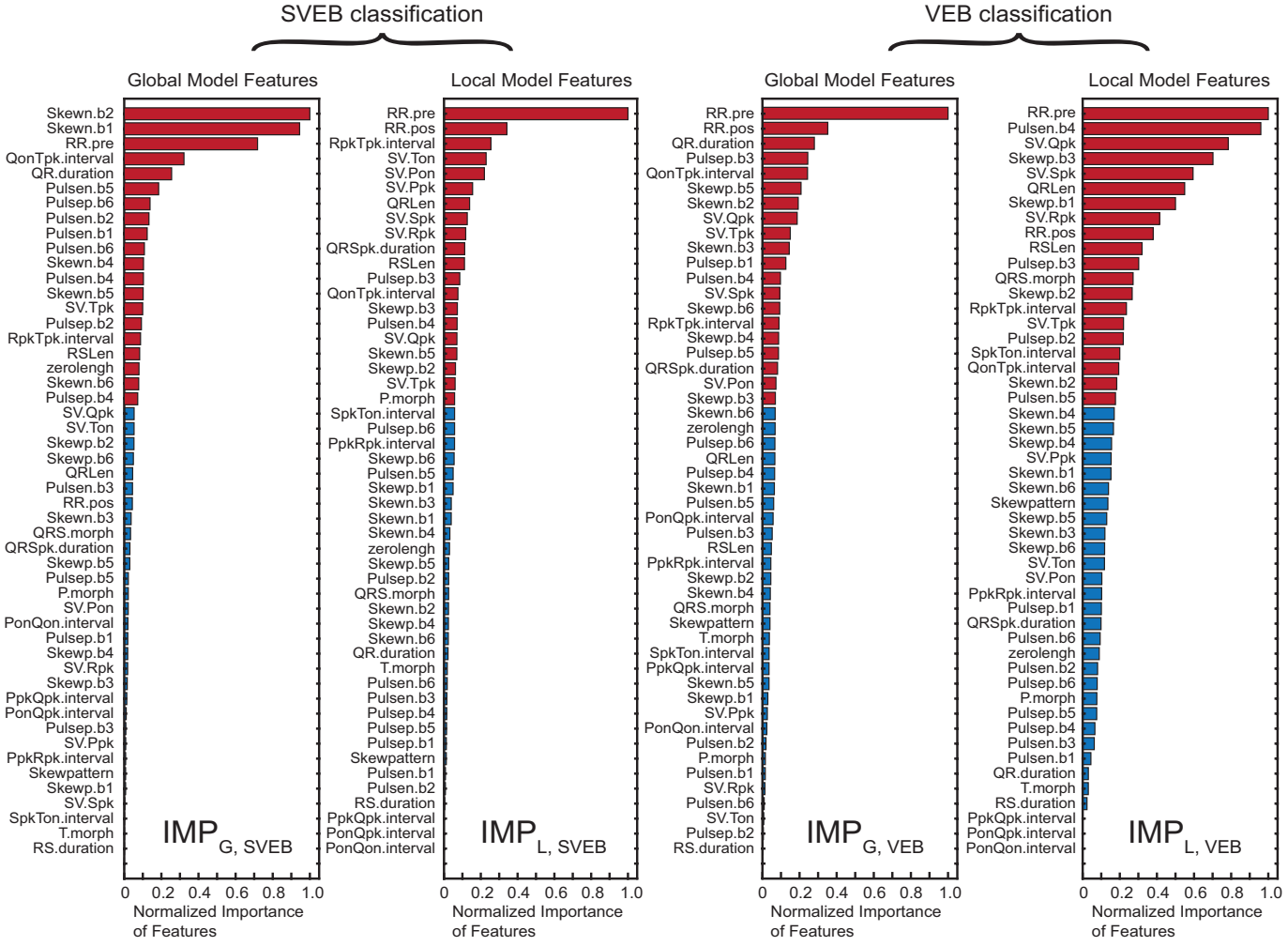

Fig. 6. Normalized feature importance for SVEB and VEB classification in global and local classifiers obtained by calculating the proposed scores IMP_G and IMP_L (the top 20 critical features are marked in red and the remaining features are marked in blue)

and local classifiers. For VEB classification, the number of the same features between the global and local classifiers are nine in the top 20 and three in the top 10 critical features. This indicates that VEB has less interpatient difference than SVEB.

The analysis of feature importance using the proposed scores provides important information for designing future arrhythmia classification systems. For example, a more precise RR interval detection circuit can be utilized for improving the system classification since such a feature is very important as shown by the above analysis. On the contrary, some feature extraction circuits related to a few less important features can be discarded to save power and further prolong the battery lifetime. Moreover, the analysis of feature importance can

be exploited to design targeted specific arrhythmia detection systems by identifying some crucial features, such as detecting ventricular flutter or fibrillation that are vital to human lives. Due to the page limit, these interesting topics are beyond the scope of this paper. They are left for our future investigation.

VI. Discussion

TABLE V
MAJOR DIFFERENCE BETWEEN PRIOR WORKS AND THE PROPOSED EDAC SYSTEM

Core Function	QRS detection	AGC	Delineation	Feature extraction		Arrhythmia Classification
				Morphology	Timing	
Prior work [32]	✔	✖	✖	✔	✖	✖
Prior work [33]	✔	✖	✔	✖	✔	✖
Prior work [34]	✖	✖	✖	✔	✖	✔
This work	✔	✔	✔	✔	✔	✔

The proposed near-sensor EDAC system can report delineated ECG information and VEB and SVEB warnings. Compared with prior works, it can achieve all targeted functions as shown in Table. V. Moreover, it has potential to be integrated within future ECG monitoring biosensors. Although it has been proven for its performance with an amplitude-varied ECG input and resilience to baseline wandering, the proposed system is still a prototype, and the biosensor scenario faces more complicated environment issues that may limit system performance, such as EMG, movement noise, and other interferences. Several schemes have been proposed focusing on wearable ECG detection under noise [51]–[54], ECG signal quality assessment [55], and noise suppression [56], [57], and this topic will also be investigated in the future. Also based with a more experimental analysis, we plan to make the system more robust to wearable applications. Low-power analog front-end circuit (below 100 nW) [58], [59] to be integrated in the EDAC system is also in our future research plan. Moreover, based on the features importance analysis, lower hardware cost arrhythmia classification algorithms (μW level) can be implemented more efficiently.

VII. Conclusion

This paper has presented an ECG delineation and arrhythmia classification (EDAC) system for wearable ECG biosensors. Using the proposed analog to feature converter (AFC) and automatic gain control (AGC) blocks, the EDAC system combines the advantages of prior works and improved the data quality for arrhythmia classification. The system has achieved a comprehensive extraction of high-quality features for ECG signals with large amplitude variations by generating a 50-element feature vector that includes both morphology and timing features. These advantages benefit the subsequent arrhythmia classification when using a patient-dependent SVM classifier. The evaluation results show that compared to existing designs, the EDAC system provides a comprehensive and better classification performance while maintaining low power and low complexity hardware. Two feature importance scores have been defined in this paper for analyzing the importance of different ECG features when performing arrhythmia classification. An improved classification algorithm that considers such feature importance analysis and the related system design/system-on-chip implementation are left for future work.

References

[1] "Cardiovascular diseases (CVDs)." [Online]. Available: https://www.who.int/en/news-room/fact-sheets/detail/cardiovascular-diseases-(cvds)

[2] S. S. Virani, A. Alonso, H. J. Aparicio, E. J. Benjamin, M. S. Bittencourt, C. W. Callaway, A. P. Carson, A. M. Chamberlain, S. Cheng, F. N. Delling *et al.*, "Heart disease and stroke statistics—2021 update: a report from the American Heart Association," *Circulation*, vol. 143, no. 8, pp. e254–e743, 2021.

[3] L. Su, S. Borov, and B. Zrenner, "12-lead Holter electrocardiography," *Herzschrittmachertherapie+ Elektrophysiologie*, vol. 24, no. 2, pp. 92–96, 2013.

[4] J. Gómez-Clapers and R. Casanella, "A fast and easy-to-use ECG acquisition and heart rate monitoring system using a wireless steering wheel," *IEEE Sensors Journal*, vol. 12, no. 3, pp. 610–616, 2011.

[5] B. M. Li, A. C. Mills, T. J. Flewwellin, J. L. Herzberg, A. S. Bosari, M. Lim, Y. Jia, and J. S. Jur, "Influence of Armband Form Factors on Wearable ECG Monitoring Performance," *IEEE Sensors Journal*, vol. 21, no. 9, pp. 11 046–11 060, 2021.

[6] S. Masihi, M. Panahi, D. Maddipatla, A. J. Hanson, S. Fenech, L. Bonek, N. Sapoznik, P. D. Fleming, B. J. Bazuin, and M. Z. Atashbar, "Development of a Flexible Wireless ECG Monitoring Device with Dry Fabric Electrodes for Wearable Applications," *IEEE Sensors Journal*, 2021.

[7] S. Yin, N. Xue, C. You, Y. Guo, P. Yao, Y. Shi, T. Liu, L. Yao, J. Zhou, J. Sun *et al.*, "Wearable Physiological Multi-Vital Sign Monitoring System With Medical Standard," *IEEE Sensors Journal*, vol. 21, no. 23, pp. 27 157–27 167, 2021.

[8] B. M. G. Rosa, S. Anastasova-Ivanova, and G. Z. Yang, "NFC-Powered flexible chest patch for fast assessment of cardiac, hemodynamic, and endocrine parameters," *IEEE Transactions on Biomedical Circuits and Systems*, vol. 13, no. 6, pp. 1603–1614, 2019.

[9] J. Wannenburg, R. Malekian, and G. P. Hancke, "Wireless capacitive-based ECG sensing for feature extraction and mobile health monitoring," *IEEE Sensors Journal*, vol. 18, no. 14, pp. 6023–6032, 2018.

[10] C. Buaban, C. Ratametha, T. Limpisawas, T. Songthawornpong, B. Pholpoke, and W. Wattanapanitch, "A Low-Power High-Input-Impedance ECG Readout System Employing a Very High-Gain Amplification and a Signal-Folding Technique for Dry-Electrode Recording," *IEEE Sensors Journal*, vol. 21, no. 17, pp. 18 905–18 919, 2021.

[11] V. P. Rachim and W.-Y. Chung, "Wearable noncontact armband for mobile ECG monitoring system," *IEEE Transactions on Biomedical Circuits and Systems*, vol. 10, no. 6, pp. 1112–1118, 2016.

[12] X. Zhang, Z. Zhang, Y. Li, C. Liu, Y. X. Guo, and Y. Lian, "A 2.89-μW Dry-Electrode Enabled Clockless Wireless ECG SoC for Wearable Applications," *IEEE Journal of Solid-State Circuits*, vol. 51, no. 10, pp. 2287–2298, 2016.

[13] W. Bai, Z. Zhu, Y. Li, and L. Liu, "A 64.8 μW >2.2 GΩ DC-AC configurable CMOS front-end IC for wearable ECG monitoring," *IEEE Sensors Journal*, vol. 18, no. 8, pp. 3400–3409, 2018.

[14] S. M. Abubakar, M. R. Khan, W. Saadeh, and M. A. B. Altaf, "A wearable auto-patient adaptive ECG processor for shockable cardiac arrhythmia," in *2018 IEEE Asian Solid-State Circuits Conference (A-SSCC)*. IEEE, 2018, pp. 267–268.

[15] K. H. Lee and N. Verma, "A low-power processor with configurable embedded machine-learning accelerators for high-order and adaptive analysis of medical-sensor signals," *IEEE Journal of Solid-State Circuits*, vol. 48, no. 7, pp. 1625–1637, 2013.

[16] A. Ukil, L. Marin, S. C. Mukhopadhyay, and A. J. Jara, "AFSense-ECG: Atrial Fibrillation Condition Sensing from Single Lead Electrocardiogram (ECG) Signals," *IEEE Sensors Journal*, 2022.

[17] A. Y. Hannun, P. Rajpurkar, M. Haghpanahi, G. H. Tison, C. Bourn, M. P. Turakhia, and A. Y. Ng, "Cardiologist-level arrhythmia detection and classification in ambulatory electrocardiograms using a deep neural network," *Nature Medicine*, vol. 25, no. 1, pp. 65–69, 2019.

[18] S. S. Xu, M.-W. Mak, and C.-C. Cheung, "Towards end-to-end ECG classification with raw signal extraction and deep neural networks," *IEEE Journal of Biomedical and Health Informatics*, vol. 23, no. 4, pp. 1574–1584, 2018.

[19] S. Saadatnejad, M. Oveisi, and M. Hashemi, "LSTM-based ECG classification for continuous monitoring on personal wearable devices," *IEEE Journal of Biomedical and Health Informatics*, vol. 24, no. 2, pp. 515–523, 2019.

[20] D. Lai, X. Fan, Y. Zhang, and W. Chen, "Intelligent and efficient detection of life-threatening ventricular arrhythmias in short segments of surface ECG signals," *IEEE Sensors Journal*, vol. 21, no. 13, pp. 14 110–14 120, 2020.

[21] E. Besler, P. K. Mathur, H. C. Gay, R. S. Passman, and A. V. Sahakian, "Inter-Patient Atrial Flutter Classification Using FFT-Based Features and a Low-Variance Stacking Classifier," *IEEE Transactions on Biomedical Engineering*, vol. 69, no. 1, pp. 156–164, 2021.

[22] M. Dey, N. Omar, and M. A. Ullah, "Temporal Feature-Based Classification Into Myocardial Infarction and Other CVDs Merging CNN and Bi-LSTM From ECG Signal," *IEEE Sensors Journal*, vol. 21, no. 19, pp. 21 688–21 695, 2021.

[23] E. Prabhakararao and S. Dandapat, "Myocardial infarction severity stages classification from ecg signals using attentional recurrent neural network," *IEEE Sensors Journal*, vol. 20, no. 15, pp. 8711–8720, 2020.

[24] T. Pokaprakarn, R. R. Kitzmiller, R. Moorman, D. E. Lake, A. K. Krishnamurthy, and M. Kosorok, "Sequence to Sequence ECG Cardiac Rhythm Classification using Convolutional Recurrent Neural Networks," *IEEE Journal of Biomedical and Health Informatics*, 2021.

[25] Q. Cai, X. Xu, Y. Zhao, L. Ying, Y. Li, and Y. Lian, "A 1.3 μW Event-Driven ANN Core for Cardiac Arrhythmia Classification in Wearable Sensors," *IEEE Transactions on Circuits and Systems II: Express Briefs*, vol. 68, no. 9, pp. 3123–3127, 2021.

[26] N. Wang, J. Zhou, G. Dai, J. Huang, and Y. Xie, "Energy-efficient intelligent ECG monitoring for wearable devices," *IEEE Transactions on Biomedical Circuits and Systems*, vol. 13, no. 5, pp. 1112–1121, 2019.

[27] K. Karboub, M. Tabaa, F. Monteiro, S. Dellagi, F. Moutaouakkil, and A. Dandache, "Automated Diagnosis System for Outpatients and Inpatients With Cardiovascular Diseases," *IEEE Sensors Journal*, vol. 21, no. 2, pp. 1935–1946, 2020.

[28] X. Bian, W. Xu, Y. Wang, L. Lu, and S. Wang, "Direct Feature Extraction and Diagnosis of ECG Signal in the Compressed Domain," *IEEE Sensors Journal*, vol. 21, no. 15, pp. 17 096–17 106, 2021.

[29] J. Yang and R. Yan, "A Multidimensional Feature Extraction and Selection Method for ECG Arrhythmias Classification," *IEEE Sensors Journal*, vol. 21, no. 13, pp. 14 180–14 190, 2020.

[30] Q. Li, C. Rajagopalan, and G. D. Clifford, "Ventricular fibrillation and tachycardia classification using a machine learning approach," *IEEE Transactions on Biomedical Engineering*, vol. 61, no. 6, pp. 1607–1613, 2013.

[31] A. Kumar, R. Ranganatham, M. Kumar, and R. Komaragiri, "Hardware emulation of a biorthogonal wavelet transform-based heart rate monitoring device," *IEEE Sensors Journal*, vol. 21, no. 4, pp. 5271–5281, 2020.

[32] X. Tang, Q. Hu, and W. Tang, "A real-time QRS detection system with PR/RT interval and ST segment measurements for wearable ECG sensors using parallel delta modulators," *IEEE Transactions on Biomedical Circuits and Systems*, vol. 12, no. 4, pp. 751–761, 2018.

[33] X. Tang and W. Tang, "A 151nw second-order ternary delta modulator for ecg slope variation measurement with baseline wandering resilience," in *2020 IEEE Custom Integrated Circuits Conference (CICC)*. IEEE, 2020, pp. 1–4.

[34] X. Tang, Z. Ma, Q. Hu, and W. Tang, "A real-time arrhythmia heartbeats classification algorithm using parallel delta modulations and rotated linear-kernel support vector machines," *IEEE Transactions on Biomedical Engineering*, vol. 67, no. 4, pp. 978–986, 2019.

[35] G. B. Moody and R. G. Mark, "The impact of the MIT-BIH arrhythmia database," *IEEE Engineering in Medicine and Biology Magazine*, vol. 20, no. 3, pp. 45–50, 2001.

[36] A. L. Goldberger, L. A. Amaral, L. Glass, J. M. Hausdorff, P. C. Ivanov, R. G. Mark, J. E. Mietus, G. B. Moody, C.-K. Peng, and H. E. Stanley, "PhysioBank, PhysioToolkit, and PhysioNet: components of a new research resource for complex physiologic signals," *Circulation*, vol. 101, no. 23, pp. e215–e220, 2000.

[37] A. S. Alvarado, C. Lakshminarayan, and J. C. Principe, "Time-based compression and classification of heartbeats," *IEEE Transactions on Biomedical Engineering*, vol. 59, no. 6, p. 1641, 2012.

[38] Association for the Advancement of Medical Instrumentation and others, "Testing and reporting performance results of cardiac rhythm and ST segment measurement algorithms," *ANSI/AAMI EC38*, vol. 1998, 1998.

[39] P. de Chazal and R. B. Reilly, "A patient-adapting heartbeat classifier using ECG morphology and heartbeat interval features," *IEEE Transactions on Biomedical Engineering*, vol. 53, no. 12, pp. 2535–2543, 2006.

[40] P. Li, Y. Wang, J. He, L. Wang, Y. Tian, T.-s. Zhou, T. Li, and J.-s. Li, "High-performance personalized heartbeat classification model for long-term ECG signal," *IEEE Transactions on Biomedical Engineering*, vol. 64, no. 1, pp. 78–86, 2017.

[41] A. Amirshahi and M. Hashemi, "ECG classification algorithm based on STDP and R-STDP neural networks for real-time monitoring on ultra low-power personal wearable devices," *IEEE Transactions on Biomedical Circuits and Systems*, vol. 13, no. 6, pp. 1483–1493, 2019.

[42] S. S. Xu, M.-W. Mak, and C.-C. Cheung, "I-vector-based patient adaptation of deep neural networks for automatic heartbeat classification," *IEEE Journal of Biomedical and Health Informatics*, vol. 24, no. 3, pp. 717–727, 2019.

[43] J. Malik, O. C. Devecioglu, S. Kiranyaz, T. Ince, and M. Gabbouj, "Real-Time Patient-Specific ECG Classification by 1D Self-Operational Neural Networks," *IEEE Transactions on Biomedical Engineering*, vol. 69, no. 5, pp. 1788–1801, 2022.

[44] X. Tang and W. Tang, "An ECG Delineation and Arrhythmia Classification System using Slope Variation Measurement by Ternary SecondOrder Delta Modulators for Wearable ECG Sensors," *IEEE Transactions on Biomedical Circuits and Systems*, 2021.

[45] S. Yin, M. Kim, D. Kadetotad, Y. Liu, C. Bae, S. J. Kim, Y. Cao, and J.-s. Seo, "A 1.06-μ W Smart ECG Processor in 65-nm CMOS for Real-Time Biometric Authentication and Personal Cardiac Monitoring," *IEEE Journal of Solid-State Circuits*, vol. 54, no. 8, pp. 2316–2326, 2019.

[46] J. M. Bote, J. Recas, F. Rincón, D. Atienza, and R. Hermida, "A modular low-complexity ECG delineation algorithm for real-time embedded systems," *IEEE Journal of Biomedical and Health Informatics*, vol. 22, no. 2, pp. 429–441, 2017.

[47] Z. Chen, J. Luo, K. Lin, J. Wu, T. Zhu, X. Xiang, and J. Meng, "An energy-efficient ECG processor with weak-strong hybrid classifier for arrhythmia detection," *IEEE Transactions on Circuits and Systems II: Express Briefs*, vol. 65, no. 7, pp. 948–952, 2017.

[48] Y. H. Hu, S. Palreddy, and W. J. Tompkins, "A patient-adaptable ECG beat classifier using a mixture of experts approach," *IEEE Transactions on Biomedical Engineering*, vol. 44, no. 9, pp. 891–900, 1997.

[49] T. Ince, S. Kiranyaz, and M. Gabbouj, "A generic and robust system for automated patient-specific classification of ECG signals," *IEEE Transactions on Biomedical Engineering*, vol. 56, no. 5, pp. 1415–1426, 2009.

[50] S. Kiranyaz, T. Ince, and M. Gabbouj, "Real-time patient-specific ECG classification by 1-D convolutional neural networks," *IEEE Transactions on Biomedical Engineering*, vol. 63, no. 3, pp. 664–675, 2015.

[51] M. U. Zahid, S. Kiranyaz, T. Ince, O. C. Devecioglu, M. E. Chowdhury, A. Khandakar, A. Tahir, and M. Gabbouj, "Robust R-Peak Detection in Low-Quality Holter ECGs Using 1D Convolutional Neural Network," *IEEE Transactions on Biomedical Engineering*, vol. 69, no. 1, pp. 119–128, 2021.

[52] Y. Bu, M. F. U. Hassan, and D. Lai, "The Embedding of Flexible Conductive Silver-Coated Electrodes into ECG Monitoring Garment for Minimizing Motion Artefacts," *IEEE Sensors Journal*, vol. 21, no. 13, pp. 14 454–14 465, 2020.

[53] D. Lai, Y. Bu, Y. Su, X. Zhang, and C.-S. Ma, "A flexible multilayered dry electrode and assembly to single-lead ECG patch to monitor atrial fibrillation in a real-life scenario," *IEEE Sensors Journal*, vol. 20, no. 20, pp. 12 295–12 306, 2020.

[54] C. Lin, C.-H. Yeh, C.-Y. Wang, W. Shi, B. M. F. Serafico, C.-H. Wang, C.-H. Juan, H.-W. V. Young, Y.-J. Lin, H.-M. Yeh *et al.*, "Robust fetal heart beat detection via R-peak intervals distribution," *IEEE Transactions on Biomedical Engineering*, vol. 66, no. 12, pp. 3310–3319, 2019.

[55] L. Smital, C. R. Haider, M. Vitek, P. Leinveber, P. Jurak, A. Nemcova, R. Smisek, L. Marsanova, I. Provaznik, C. L. Felton *et al.*, "Real-time quality assessment of long-term ECG signals recorded by wearables in free-living conditions," *IEEE Transactions on Biomedical Engineering*, vol. 67, no. 10, pp. 2721–2734, 2020.

[56] J. Lázaro, N. Reljin, M.-B. Hossain, Y. Noh, P. Laguna, and K. H. Chon, "Wearable armband device for daily life electrocardiogram monitoring," *IEEE Transactions on Biomedical Engineering*, vol. 67, no. 12, pp. 3464–3473, 2020.

[57] N. T. Bui, D. T. Phan, T. P. Nguyen, G. Hoang, J. Choi, Q. C. Bui, and J. Oh, "Real-time filtering and ECG signal processing based on dual-core digital signal controller system," *IEEE Sensors Journal*, vol. 20, no. 12, pp. 6492–6503, 2020.

[58] C. Sawigun and S. Thanapitak, "A Compact Sub-μW CMOS ECG Amplifier With 57.5-MΩ Z in, 2.02 NEF, 8.16 PEF and 83.24-dB CMRR," *IEEE Transactions on Biomedical Circuits and Systems*, vol. 15, no. 3, pp. 549–558, 2021.

[59] X. Yang, J. Xu, M. Ballini, H. Chun, M. Zhao, X. Wu, C. Van Hoof, C. M. Lopez, and N. Van Helleputte, "A 108 dB DR $\Delta\Sigma$-ΣM Front-End With 720 mV pp Input Range and¿$\pm$300 mV Offset Removal for Multi-Parameter Biopotential Recording," *IEEE Transactions on Biomedical Circuits and Systems*, vol. 15, no. 2, pp. 199–209, 2021.